ACS EARTH AND SPACE CHEMISTRY

http://pubs.acs.org/journal/aesccq

Article

Time-Resolved Examination of Fungal Selenium Redox Transformations

Cara M. Santelli,* Mary C. Sabuda, and Carla E. Rosenfeld

Cite This: *ACS Earth Space Chem.* 2023, 7, 960−971

Read Online

ACCESS | Metrics & More | Article Recommendations | Supporting Information

ABSTRACT: Selenium (Se) is both a micronutrient required for most life and an element of environmental concern due to its toxicity at high concentrations, and both bioavailability and toxicity are largely influenced by the Se oxidation state. Environmentally relevant fungi have been shown to aerobically reduce Se(IV) and Se(VI), the generally more toxic and bioavailable Se forms. The goal of this study was to shed light on fungal Se(IV) reduction pathways and biotransformation products over time and fungal growth stages. Two Ascomycete fungi were grown with moderate (0.1 mM) and high (0.5 mM) Se(IV) concentrations in batch culture over 1 month. Fungal growth was measured throughout the experiments, and aqueous and biomass-associated Se was quantified and speciated using analytical geochemistry, transmission electron microscopy (TEM), and synchrotron-based X-ray absorption spectroscopy (XAS) approaches. The results show that Se transformation products were largely Se(0) nanoparticles, with a smaller proportion of volatile, methylated Se compounds and Se-containing amino acids. Interestingly, the relative proportions of these products were consistent throughout all fungal growth stages, and the products appeared stable over time even as growth and Se(IV) concentration declined. This time-series experiment showing different biotransformation products throughout the different growth phases suggests that multiple mechanisms are responsible for Se detoxification, but some of these mechanisms might be independent of Se presence and serve other cellular functions. Knowing and predicting fungal Se transformation products has important implications for environmental and biological health as well as for biotechnology applications such as bioremediation, nanobiosensors, and chemotherapeutic agents.

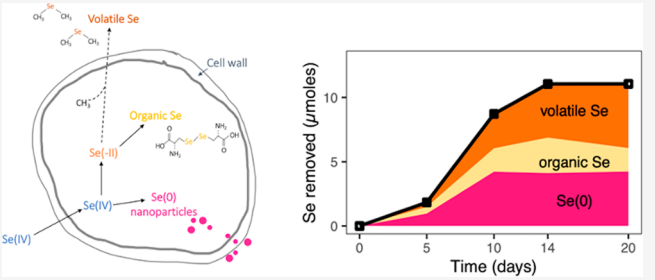

KEYWORDS: *fungi, selenite reduction, time series, redox, Se nanoparticles, organic Se, bioremediation*

1. INTRODUCTION

Selenium (Se) is both a micronutrient required for most life, particularly for the biosynthesis of selenocysteine (the 21st proteinogenic amino acid), and an element of environmental concern due to its toxicity at higher concentrations. Selenium can exist in numerous chemical forms, and both bioavailability and toxicity are heavily influenced by Se oxidation state. In the environment, Se typically exists as either organic or inorganic Se(-II), elemental Se(0), or Se(IV/VI) oxyanions. Diverse bacteria, archaea, and eukarya drive Se redox reactions[1−7] as well as selenoprotein biosynthesis and methylation reactions.[8−13] Selenite, Se(IV), and selenate, Se(VI), can be toxic to many organisms. The reduction of these oxyanions to Se(0) and Se(-II) potentially serves as a detoxification strategy, as Se(0) has been shown to be biocompatible and subtoxic[14−16] and Se(-II) can be methylated to form low-toxicity compounds or compounds that can be volatilized to reduce total Se levels.[9,17−19] Organoselenium biosynthesis can also be highly beneficial for organisms, as these compounds generally perform a variety of useful cellular functions such as protection against and recovery from oxidative stress.[20,21]

Recent studies have shown that numerous Ascomycete fungi can tolerate and grow in high Se concentrations (>10 mM) in aqueous and soil environments.[2,22−27] Further, these fungi are capable of Se redox and biotransformation reactions such as Se(IV) and Se(VI) reduction to various reduced Se forms. These biotransformation products are largely red, amorphous Se(0) nanoparticles (SeNPs) and volatile methylated compounds such as dimethylselenide and dimethyldiselenide.[2,9,28−31] Some fungi may also produce intracellular organoselenium compounds similar to selenoproteins or selenoamino acids produced by bacteria and other higher organisms.[32−34] Until recently, it was thought that fungi did not have the genetic machinery (e.g., Sec synthesis and insertion) to form selenocysteine and related selenoproteins[35,36] A 2019 study by Mariotti et al.,[37] however, showed

Special Issue: Environmental Redox Processes and Contaminant and Nutrient Dynamics

Received: September 18, 2022
Revised: April 21, 2023
Accepted: April 24, 2023
Published: May 5, 2023

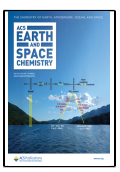

that early branching fungal phyla do contain selenoprotein synthesis genes, but these genes were lost by Ascomycota (the phylum of which the fungi in this study belong) and Basidiomycota. The formation of these organoselenium compounds in these fungal phyla must proceed through alternative synthesis pathways, potentially via Se substitution for S in related compounds (e.g., methionine is converted to selenomethionine),[38−40] but these pathways and compounds are poorly resolved in fungi.

Many questions remain about how quickly Se is reduced by different species of fungi, whether the reduction rate is constant over time or changes with decreasing dissolved Se concentrations, if and how Se biotransformation products change with time, and how these biotransformation rates and products relate to different fungal growth phases. Active metabolites during exponential growth likely differ from those produced in later growth stages,[41−43] and may impact fungal mediation of certain Se transformation reactions. This has been observed previously in several Ascomycete fungi, where the metabolites putatively responsible for Mn(II) oxidation changed with time and fungal growth.[44] Although earlier studies showed Ascomycete fungi could promote Se(VI) reduction, the concentrations under which SeNPs were observed were not environmentally relevant for most fungal species and the diversity of biotransformation products appeared fewer than for Se(IV) reduction.[2] Thus, experiments in this study were conducted to specifically address multiple unknowns about Se(IV) reduction and to shed light on fungal Se(IV) reduction pathways and biotransformation products over time and fungal growth stages. Specifically, *Alternaria alternata* strain SRC1lrK 2f and *Paraphaeosphaeria sporulosa* strain AP 3s5-JAC2a were grown with 0.1 mM (moderate) and 0.5 mM (high) Se(IV) concentrations in batch culture experiments over 32 days. Fungal growth was measured throughout the experiments, and aqueous and biomass-associated Se was quantified and speciated using analytical geochemistry, transmission electron microscopy (TEM), and synchrotron-based X-ray absorption spectroscopy (XAS) approaches. These two fungal species were selected because previous studies that examined only the experiment's end points showed these species to have substantially different Se(IV) toxicity responses and levels of Se transformation products depending on growth conditions, nutrient sources, and timing of Se exposure (e.g, concurrent with or after exponential growth).[2,23,45] Understanding how these different Se pools evolve over time, decreasing Se(IV) concentration, and fungal growth in the presence of Se is important, especially if one phase is preferred over another for specific applications. Results will provide more insight into the Se(IV) reduction pathways, rates, and diverse Se biotransformation products employed by these environmentally relevant fungi as well as provide greater constraints for technological applications, such as designing an effective fungal bioreactor for remediating Se-impacted environments.

2. MATERIALS AND METHODS

2.1. Culture Experiments. Pure culture, liquid batch experiments of two previously isolated[46,47] fungal isolates, *Alternaria alternata* strain SRC1lrK2f and *Paraphaeosphaeria sporulosa* (previously called *Paraconiothyrium sporulosum*) strain AP3s5-JAC2a, were conducted over 32 days to examine the fungal response to Se(IV) exposure over time. These isolates have been shown to remove aqueous Se(IV) from solution through Se reduction pathways.[2,23,32,45] Prior to the start of the experiment, a fungal stock culture for each isolate was grown for approximately 2 weeks in 100 mL of liquid HEPES-buffered (20 mM, pH = 7) AY media (adapted from Miyata et al.,[48] as described in Rosenfeld et al.[2]) without Se in sterile 250 mL Erlenmeyer flasks. After the two week growth period, fungal stock cultures were blended for 30 s in a presterilized metal blender to break the biomass into more uniform size fractions immediately prior to the experiment start. To initiate each experiment, 100 μL of blended fungal stock culture (biomass weight was below detection on the analytical balance) was added to sterile 250 mL Erlenmeyer flasks filled with 100 mL of fresh AY media supplemented with 0.1 mM (10 μmol) Se(IV) or 0.5 mM (50 μmol) Se(IV). All experiments were conducted at room temperature (~21 °C) in the dark without agitation, as previous work with these cultures showed growth sensitivity to quickly stirred conditions.[49] At each of 5 sampling points (5, 10, 14, 20, 32 days), replicate cultures were individually filtered through a preweighed 0.22 μm methyl cellulose ester (MCE) filter to determine the quantity of Se remaining in solution and associated with the solid phase. Additional replicate cultures were also sampled at each time point for transmission electron microscopy (TEM) and synchrotron-based X-ray absorption spectroscopy (XAS). For TEM, fungal biomass was sampled and chemically fixed using glutaraldehyde, as described below. For XAS, all biomass and extracellular precipitates were scraped from the flask surfaces and vacuum filtered using a 0.22 μm MCE filter to collect the biomass and extracellular precipitates. Filtered biomass was packed as a wet paste on top of the membrane filter, sealed in Kapton tape to avoid desiccation, and immediately frozen at −20 °C to stop fungal growth and further redox reactions. Previous experiments in our lab suggest that −20 °C is sufficient for longer term storage and preserving Se geochemistry against further transformation.[2,32,35]

For a biological control, the fungi were also grown without Se to assess fungal growth unaffected by the presence of Se. Two additional control experiments were performed to examine abiotic factors influencing Se geochemistry. For one abiotic control, biomass-free flasks containing only Se(IV)-amended media were established in triplicate and sampled at each time point. Killed-biomass controls were also conducted to assess potential abiotic Se adsorption to the fungal biomass. For these, a fungal stock flask was cultured for approximately 2 weeks in AY media without Se before blending and inoculating 250 mL Erlenmeyer flasks as described above for the biological experiments. The fungi were then grown for 10 days in their respective flasks filled with fresh, Se-free AY media before removing the biomass and soaking in 100% ethanol overnight in sterile 50 mL falcon tubes to kill the fungus. During this time, the experimental flasks were emptied, autoclaved to ensure sterility, and refilled with fresh Se-containing media. After 24 h had elapsed, the ethanol-killed fungal biomass was transferred to the Se(IV)-containing AY media (0.1 mM or 0.5 mM) and sampled as described above. Unlike in the biotic experiments, there was no fungal growth visible (e.g., no increase in mycelium size or abundance) in the killed-biomass controls. No unexpected or unusually high safety hazards were encountered during these experiments or analyses described below.

2.2. Analytical Methods. *2.2.1. Quantitative Aqueous Phase Chemistry.* Se remaining in the aqueous phase was

https://doi.org/10.1021/acsearthspacechem.2c00288
ACS Earth Space Chem. 2023, 7, 960−971

analyzed via ion chromatography as described previously.[2] Briefly, triplicate flasks were filtered onto a preweighed 0.22 μm MCE filter to collect biomass, and the filtrate was collected in a sterile 50 mL Falcon tube and stored at 4 °C until analysis. While 0.1 mM Se(IV) samples did not require dilution, immediately before analysis, 0.5 mM Se(IV) samples were diluted 1:10 with ultrapure (18 mΩ - cm) water, and all samples were run on an ion chromatograph (Metrohm Professional IC Vario 1 AnCat) optimized for Se(IV and VI) analysis. The limit of detection was 0.001 mM for each anion and the precision was measured to 3 decimal places.

2.2.2. Fungal Growth and Solid-Associated Se. To assess fungal growth throughout the experiment and to determine the amount of solid-associated Se, the biomass collected on each preweighed MCE filter was air-dried and weighed at each sampling point. The filter weight (measured to 4 decimal places) was subtracted to obtain the fungal biomass. After weighing, samples were acid digested as described previously.[2,23,32] Briefly, biomass and any solid-associated Se was digested overnight at room temperature in 0.5 mL hydrogen peroxide and 4.5 mL concentrated trace metal grade nitric acid in 30 mL PFA bottles. Samples were then diluted to appropriate concentrations for analysis via inductively coupled plasma optical emission spectrometry (ICP-OES; Thermo iCAP 6000) at the Analytical Geochemistry Lab at the University of Minnesota. The limit of detection for this instrument was 0.01 mg/L. Ultrapure water blanks and clean MCE filters were also digested, acidified, and analyzed as described above for quality control, which showed no measurable Se.

2.2.3. Mass Balance Calculations. While volatile Se forms could not be captured and detected due to the nature of these culturing methods (i.e., atmospheric gas exposure), a mass balance calculation was performed to approximate the amount of Se potentially volatilized (missing) from each culture. At each sampling point, the amount of Se remaining in solution and the amount of Se associated with the solid phase were converted to μmoles and subtracted from the initial amount of Se added (0.1 and 0.5 mM Se(IV); 10 and 50 μmoles respectively).

2.2.4. Transmission Electron Microscopy (TEM). At each sampling point, a small amount of biomass was preserved in 2.5% glutaraldehyde and subjected to an ethanol dehydration series (75%, 95%, 100%) as described previously for transmission electron microscopy.[2] Briefly, desiccated samples were embedded in epoxy resin, sectioned to 50 nm with a Leica UC6 ultramicrotome, and mounted on 100 mesh Cu grids. Section duplicates were either stained with 2% uranyl acetate or left unstained. Stained sections were imaged at 80 kV with a FEI Tecnai G2 Spirit BioTWIN and 120 kV on a FEI Tecnai G2 F30 to avoid burning through any Se nanoparticles. To examine the chemical composition of the particles and cellular material, unstained sections were imaged at 120 kV with a FEI Tecnai T12 equipped with an Oxford Inca energy dispersive X-ray spectrometer (EDS). TEM was conducted in the University of Minnesota Characterization Facility.

2.2.5. Synchrotron-Based X-ray Absorption Spectroscopy. X-ray absorption spectroscopy (XAS) was performed at beamline 12-BM at the Advanced Photon Source (APS) at Argonne National Laboratory to characterize the solid-associated Se forms. All samples were shipped frozen to the APS and allowed to thaw immediately prior to analysis. Detailed XAS experiments and data analysis methods are described previously.[32] Briefly, fluorescence spectra were collected for all samples from −200 to +800 eV around the Se K-edge (12658 eV) using a Si(111) monochromator. Approximately 3 to 4 successive scans were collected from each sample, monitored to ensure no radiation-induced redox changes occurred during data collection, and averaged to obtain a single high-quality spectrum. Data reduction, normalization, and analysis of the bulk XAS data was performed using the Athena program in Demeter (version 0.9.26).[50] Solid-associated Se speciation was determined by using the extended X-ray absorption fine structure (EXAFS) region of the spectra. Principal component analysis (PCA) with a target transformation analysis (TTA) using a spectral library of model Se compounds was first performed to identify the number and fitness of relevant model compounds to our entire data set, as described previously.[49] The spectral reference library was then used to identify and quantify the structural components using linear combination fitting (LCF).[51] In the LCF approach, binding energies were fixed, negative component contributions were prohibited, and components were summed to 1.0. Goodness of fit was established by minimizing the *R* factor (normalized sum of squares; NSS) parameter. The reference library for Se included sodium selenate (Na_2SeO_4), sodium selenite (Na_2SeO_3), selenous acid (H_2SeO_3), gray crystalline Se(0), black amorphous Se(0), red amorphous Se(0) synthesized and stabilized with glucose,[52] seleno-DL-cystine (referred to herein as selenocystine or Se-cystine), Se-methyl-L-selenocysteine (referred to herein as selenocysteine), seleno-DL-methionine (referred to herein as selenomethionine or Se-methionine), iron selenide (FeSe), and zinc selenide (ZnSe).

3. RESULTS AND DISCUSSION

3.1. Fungal Growth Response and Toxicity to Selenite Exposure. Growth of filamentous Ascomycete fungi *Alternaria alternata* and *Paraphaeosphaeria sporulosa* was negatively impacted by the presence of Se(IV) at concentrations similar to those observed in industrial wastewaters with moderate to high Se levels.[23,25] Specifically, the dry biomass weights at both the moderate (0.1 mM) and high (0.5 mM) Se(IV) concentrations were lower at nearly all time points relative to growth in Se-free conditions (Figure 1; Table S1). The impact of Se(IV) exposure, however, was more pronounced for *P. sporulosa* (Figure 1) throughout the experiment, where dry biomass weights were diminished by ∼69% (moderate Se levels) and ∼77% (high Se levels) relative to Se-free growth conditions and even dropped to ∼92% lower at high Se exposure at the completion of the experiment. In comparison, *A. alternata* biomass levels (Figure 1) decreased by ∼27% to ∼36% for the moderate and high Se(IV) concentrations, respectively. It is important to note, however, that these initial Se(IV) concentrations were not maintained throughout the course of the experiment, but decreased over time (described below).

Earlier experiments with these two fungal isolates[2,45] showed a similar impact of diminished fungal growth with increased Se(IV) concentrations, as well as a more substantial negative growth effect on *P. sporulosa* compared to *A. alternata*. In previous experiments by Rosenfeld et al.,[2] fungi were grown on agar-solidified media which only allows two-dimensional radial extension (i.e., mycelial diameter) to be measured. The study by Sabuda et al.[45] and the present study assessed submerged

https://doi.org/10.1021/acsearthspacechem.2c00288
ACS Earth Space Chem. 2023, 7, 960−971

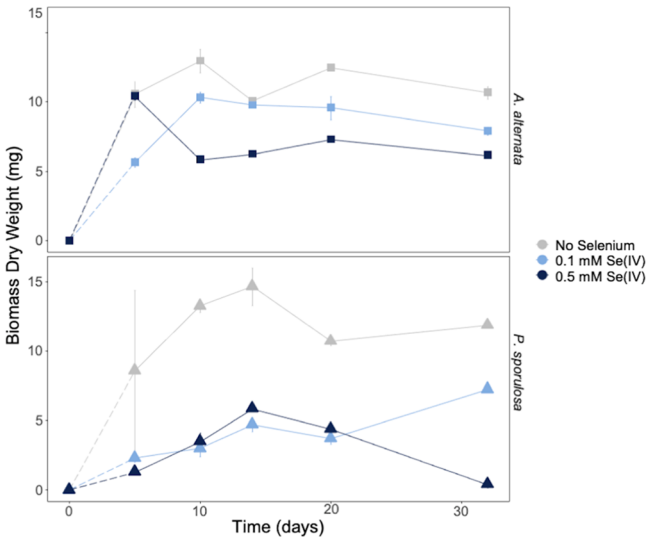

Figure 1. Net dry biomass weights (mg) for *A. alternata* (top panel) and *P. sporulosa* (bottom panel) grown in the presence of 0.1 mM Se(IV), 0.5 mM Se(IV), or no added Se. Points are averages of replicate cultures, where bars represent the range of measured values for the two replicates. Points where no bars are visible have ranges smaller than the vertical point size. Dashed lines from time point zero are inferred, as the actual biomass at the start of the experiment was too low to be measured (~0 mg at $t = 0$).

fungal growth in liquid media and therefore were able to quantify total fungal biomass throughout the experiment. This approach incorporates the complex, three-dimensional mycelial growth whereby individual hypha grow outward through apical tip expansion, and hyphal branching promotes a tree-like morphology with a fractal geometry.[53,54] Nutrient availability and myriad environmental conditions can impact the growth morphology of fungal mycelia, and a typical growth curve for filamentous fungi is not well constrained.[41,54,55] Although growth rates (biomass/day) and overall biomass quantities decreased in the presence of Se(IV), the overall shapes of the growth curves (Figure 1) were largely similar for each fungal species, regardless of Se concentration. *A. alternata* biomass increased quickly (exponential growth phase) and stagnated (i.e., reached stationary phase) within 10 days, whereas growth proceeded more slowly for *P. sporulosa,* which required ~14 days to reach stationary phase. Interestingly, average Se-free dry weights (~12 mg) during stationary phase were similar for both fungal species, suggesting that a nutrient limitation was met under these Se-free conditions, but not in Se-enriched growth conditions. Indeed, the recent study by Sabuda et al.[45] demonstrated that a similar amount of acetate (the primary carbon source used here) was depleted completely within 11 or 23 days by *P. sporulosa* and *A. alternata*, respectively. A steady decline in *P. sporulosa* biomass grown under high Se(IV) concentrations was observed after 14 days, indicating cell death and autolysis occurred, with the potential to release Se back into solution depending on the Se form inside of the cells (e.g., soluble anions or organic forms). This biomass decrease was not observed in any of the ethanol-killed mycelia control experiments (Figure S1; Table S1), which indicated that this autolysis stage was a direct result of fungal growth in the presence of Se(IV). Growth rates and biomass quantities in the present study differed from the Sabuda et al.[45] study, which did not observe an initial increase in biomass under similar nutrient conditions. That study, however, grew the fungi to high biomass levels before spiking with Se(IV) (and excess carbon) and hypothesized that the fungus was diverting energy from cell growth to cell protection and repair from exposure to Se(IV).

Here, the negative impact of Se(IV) on fungal growth, coupled with comparisons of the growth curves for the different fungal species under the different growth conditions, showed that increasing Se(IV) concentrations were increasingly toxic to the fungi. Selenite toxicity was previously observed in other studies of fungi,[2,17,23,56] and this toxicity resulted in similarly diminished biomass yields relative to growth under Se-free or low Se environments. Selenite toxicity likely resulted from interactions with intracellular thiols, producing reactive oxygen species (ROS) such as superoxide and hydrogen peroxide and inducing oxidative DNA damage.[17,57,58] The study by Letavayova et al.[17] showed that Se(IV) toxicity effects were more pronounced during the exponential growth phase of the budding yeast *Saccharomyces cerevisiae* compared with stationary phase, and DNA damage increased under increasing Se(IV) concentrations. Although there was some variability during exponential growth, *A. alternata* growth curves (Figure 1) suggested a similar toxicity effect and mechanism to yeast where growth was progressively inhibited at higher Se concentrations.[17] Conversely, *P. sporulosa* growth curves were similar during exponential growth under both moderate and high Se(IV) concentrations (Figure 1) suggesting that other toxicity mechanisms were possible for this fungal species. *P. sporulosa* could also be dedicating energy toward Se(IV) detoxification rather than biomass accumulation, as was observed in previous studies with varying carbon source and concentration.[45] Analysis of ROS and DNA damage, as well as more frequent sampling of fungal growth and Se dynamics during the exponential growth phase in future studies, would be valuable for constraining the specific mechanisms of Se(IV) toxicity in these filamentous fungi.

3.2. Removal of Aqueous Selenite with Time. Despite exponential growth ceasing within the first 2 weeks for both fungal species, continued Se(IV) removal occurred beyond exponential growth under all experimental conditions with living biomass, albeit with different removal rates depending on fungal species and Se(IV) exposure levels. Aqueous Se(IV) concentrations decreased more rapidly for *A. alternata* compared to *P. sporulosa* grown in either moderate (0.1 mM) or high (0.5 mM) Se(IV) concentrations (Figure 2; Table S2). For *A. alternata*, there was an initial lag in Se(IV) removal (i.e., concentration decreased minimally) for the first 5 days regardless of concentration, though there was a rapid increase in biomass during that time (Figure 1). After the first 5 days, Se(IV) concentrations decreased continuously throughout the remainder of the exponential growth phase and stationary growth until all Se was removed (moderate Se treatment) or the experiment was stopped (high Se treatment). The Se(IV) removal rate for the moderate Se treatment was ~1.4 μmol Se/day between days 5 and 10, with all Se(IV) removed within 14 days. Taking into consideration that the mycelial biomass also increased during this time, this removal rate equated to 0.14 μmol Se/day/mg biomass. In the high Se experiments, a total of 21.6 μmol Se(IV) was removed from solution. The Se(IV) removal rate was slightly lower in the greater Se concentration, averaging 1.2 μmol Se/day during exponential growth (5−10 d) and only ~0.7 μmol Se/day during the remainder of the experiment. However, the biomass

https://doi.org/10.1021/acsearthspacechem.2c00288
ACS Earth Space Chem. 2023, 7, 960−971

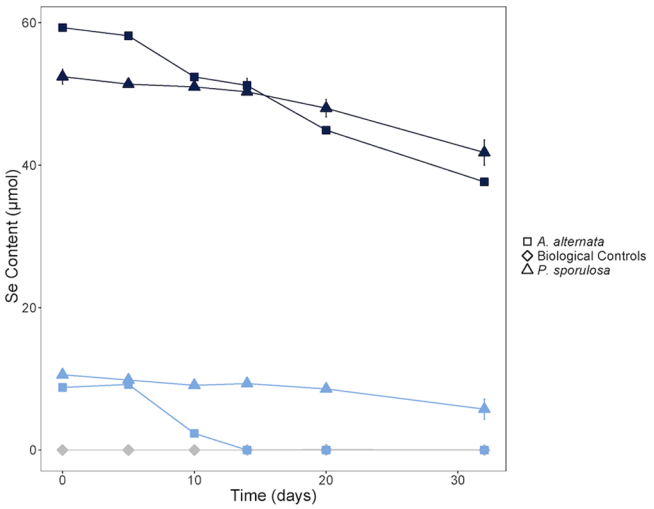

Figure 2. Aqueous Se(IV) content (μmol) remaining in solution over time for *A. alternata* (squares) and *P. sporulosa* (triangles) grown in the presence of 0.1 mM Se(IV) (light blue) and 0.5 mM Se(IV) (dark blue). Gray diamonds represent fungi grown in the absence of Se (biological controls). Points are shown as the average of the replicate cultures, where bars represent the range of measured values for the two replicates.

normalized rates were greater during exponential growth (0.21 μmol Se/day/mg biomass) and then decreased during stationary growth to 0.14 μmol Se/day/mg biomass, similar to the moderate Se conditions. This suggests that Se removal rates were dependent on several factors, including the total biomass of the fungus as well as the concentration of Se(IV) in solution, which was decreasing with time. Se was not removed from solution in the killed biomass controls (Figure S2), showing that Se removal is clearly biologically mediated.

P. sporulosa similarly promoted aqueous Se removal throughout the exponential and stationary growth phases, but the total amount removed and removal rates were substantially less than those by *A. alternata*. Only 4.8 μmol Se(IV) and 10.7 μmol Se(IV) was removed from solution under moderate and high Se conditions, respectively (Figure 2). Under both conditions, a substantial amount of Se remained in solution. The Se(IV) removal rates under moderate Se conditions were ∼0.1 μmol Se/day (0.02 μmol Se/day/mg biomass) during exponential growth phase. However, in contrast to *A. alternata,* the *P. sporulosa* removal rate increased during stationary growth to ∼0.2 μmol Se/day (0.03 μmol Se/day/mg biomass). The removal rate similarly increased in the later stages of the high Se experiments, averaging ∼0.2 μmol Se/day during the first 14 days of exponential growth and ∼0.5 μmol Se/day during the last 12 days. In this later period the total *P. sporulosa* biomass dropped significantly, suggesting cell autolysis. Normalizing these aqueous Se(IV) removal rates to biomass, of which there was substantially less *P. sporulosa* biomass than *A. alternata* biomass due to Se exposure (Figure 1), 0.034 μmol Se/day/mg biomass and 1.25 μmol Se/day/mg biomass were removed within 14 and 32 days, respectively. Increased Se removal by *P. sporulosa* under high Se conditions was unexpected, especially considering the observed autolysis and significant decrease in biomass. Depending on how the Se was transformed and stored within the cell, this catastrophic process could release Se back into solution, perhaps with varying chemical speciation (e.g., organoselenium compounds or Se(0)) that impact both toxicity and bioavailability of Se.[17,59,60] This has important implications for applications such as bioremediation where the rates of Se removal, the Se transformation products, biomass accumulation, and vitality all need to be considered together.

3.2.1. Changes in Selenium Speciation with Time. Using a mass balance approach to track and quantify Se in different pools throughout the experiment showed that aqueous Se(IV) removal occurred by multiple pathways, including immobilization (either intracellular or extracellular) and volatilization via Se(IV) reduction. As aqueous Se(IV) concentrations decreased over the course of each experiment, the amounts of solid-associated Se and volatilized Se generally increased with time, depending on fungal strain and starting Se concentration (Figure 3; Figure S3; Tables S3 and S4). When grown in

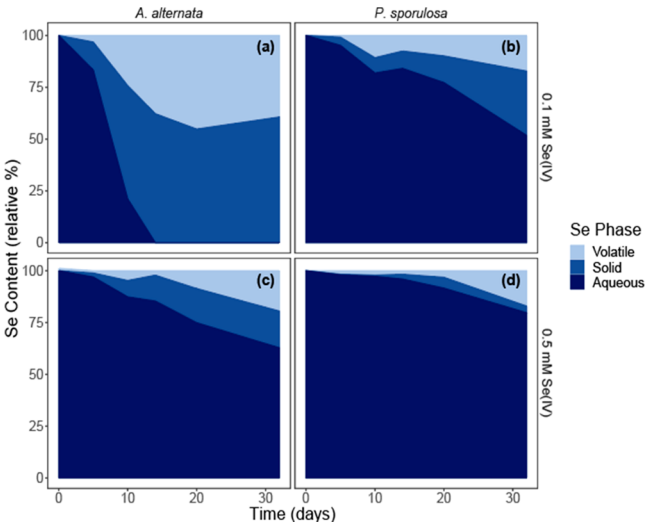

Figure 3. Relative percentages of Se pools (aqueous, solid, volatile) throughout 32 days of growth for *A. alternata* (left panels) and *P. sporulosa* (right panels) in media supplemented with (a, b) 0.1 mM Se(IV) and (c, d) 0.5 mM Se(IV), respectively.

moderate (0.1 mM) Se conditions, both *A. alternata* and *P. sporulosa* produced solid phase and volatile Se immediately after Se exposure. Initially (up to 5 days after exposure), a greater percentage of the Se was solid-associated though both volatilized Se and solid-associated Se increased substantially after initial biomass growth and continued during both exponential and stationary phase growth until all Se was depleted from solution or the experiment was completed. At high Se(IV) concentrations, there was a lag in Se volatilization, particularly for *P. sporulosa*, during which all Se transformed to the solid phase. As Se removal progressed in the experiment, the percentage of Se volatilized compared to solid-associated between the two fungal species was quite different (Figure 3). Notably, *P. sporulosa* removed most of the aqueous Se(IV) through volatilization, whereas *A. alternata* removed Se(IV) equally through volatilization and solid-producing pathways. As such, solid-associated Se was approximately 2−5 times greater for *A. alternata* compared to *P. sporulosa* (Figure S3). The greatest amount of solid-associated Se was measured for *A. alternata* grown in high Se conditions, despite its decreased biomass production (Figure 1). Increasing Se volatilization during the declining growth stage (decreasing biomass) of *P. sporulosa* was somewhat surprising but indicates that stress responses promoting Se transformation and detoxification by

https://doi.org/10.1021/acsearthspacechem.2c00288
ACS Earth Space Chem. 2023, 7, 960−971

this fungal species are complex and varied. This contrasts with an earlier study[28] that used a *Penicillium* isolate and showed steady Se volatilization throughout the different growth stages with sudden production of intracellular Se(0) only during the declining growth stage. Identifying the specific Se compounds can give insight as to whether the Se transformation mechanisms are consistent throughout the mycelial growth stages, or if the products and their relative abundances change as nutrient limitations or other stressors (e.g., Se(IV) toxicity) promote secondary metabolite formation that may impact these transformations. Volatile Se compounds were not specifically analyzed in this study, but we expect that they are primarily dimethylselenide (DMSe) based on earlier fungal Se volatilization studies.[61,62] DMSe was likely formed via Se(IV) reduction to Se(-II) and subsequent methylation of the selenide.[63,64]

The predominant solid-associated Se form (~60−90% relative abundance), based on linear combination fitting of the experimental EXAFS spectra with reference spectra of known Se compounds, was Se(0) (Figure 4; Figure S4; Table S5) regardless of experimental conditions (fungal species, initial Se concentration, growth stage). The reference library contained three different Se(0) allotropes, but the spectrum for red, amorphous Se(0) produced the best linear combination fits (Figure S4). This result was expected based on the development of a pinkish, red color of the mycelium (not shown) as well as from earlier studies[2,15,65,66] that showed biogenic Se(IV) and Se(VI) reduction produce the red, amorphous Se(0) allotrope.

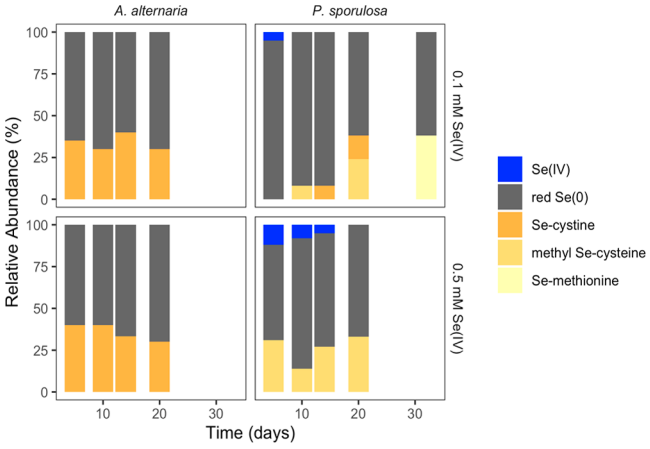

Figure 4. Relative abundance (%) of solid-associated Se species, as determined by linear combination fitting of Se K-edge EXAFS spectra, throughout 32 days of growth for *A. alternata* and *P. sporulosa* in media supplemented with 0.1 mM Se(IV) (top panels) or 0.5 mM Se(IV) (bottom panels). Selenium species shown represent those fractions >5% of total Se species. Missing data points for t = 32 days were due to flask contamination.

In addition to Se(0), a substantial portion (30−40%) of the solid-associated Se produced by *A. alternata* was selenocystine (Se-cystine), an organic selenoamino acid. *P. sporulosa* also produced selenoamino acids, but the best fits to the EXAFS spectra were predominantly methylselenocysteine (methyl Se-cysteine) (Figure 4). These fits were substantially worse with Se-cystine (>15% increases in residuals), so these compounds were likely methylselenocysteine or something highly similar. Selenomethionine (Se-methionine) was also detected at the end (day 32) of the moderate Se concentration experiment with *P. sporulosa*. Unfortunately, Se EXAFS data were not able to be collected at 32 days for any other experimental conditions due to flask contamination with bacteria, so it is unclear if the formation of this organoselenium compound is commonly formed over time as a transformation product or as a result of a switch in fungal metabolism. The spectra for Se-methionine and methyl Se-cysteine were also highly similar (Figure S4), so it is possible that EXAFS was not well suited for distinguishing between these compounds. Regardless, it is clear that different fungal species transform Se(IV) to different organoselenium products, as the monomer organoselenium fraction produced by *P. sporulosa* was distinct from the dimer Se-cystine by *A. alternata*. In other studies, similar organoselenium compounds (selenocystine, selenomethionine, and methylselenocysteine) were also produced by selenized yeast cells and confirmed using alternative analytical techniques such as high-performance liquid chromatography inductively coupled plasma mass spectrometry (HPLC-ICP-MS).[67] Previous studies of *P. sporulosa*[32] also produced organoselenium compounds with time, but exposure to both Se(IV) and Mn(II) compounds resulted in the formation of Se-cystine, whereas selenomethionine was observed when Se(VI) was substituted for Se(IV). It is unclear why these differences were observed between the studies. It is possible that Mn(II) uptake by this fungus had an impact on the Se speciation, perhaps by scavenging reactive oxygen species produced as a result of Se toxicity.[68] Regardless, the formation of both organic and inorganic Se during fungal Se(IV) reduction suggests that multiple Se detoxification and transformation mechanisms were involved, and future work would benefit from further examination of fungal organoselenium products.

Interestingly, both Se(0) and selenoamino acids (e.g., Se-cystine or methyl Se-cysteine) were detected with EXAFS after just 5 days of growth in all experiments, even though minimal (below detection) quantities of aqueous Se(IV) were removed by *P. sporulosa*. Also despite the increase in solid-associated Se concentrations (Figure S3), the relative proportions of Se(0) and selenoamino acids were fairly consistent (averaging 65%:35%) through time and the various fungal growth stages in nearly all experimental conditions (Figure 4). Only when *P. sporulosa* was grown in 0.1 mM Se(IV) was there a clear shift in solid-associated Se speciation. Under these conditions, only inorganic Se (primarily Se(0)) was initially observed, with increasing selenoamino acid abundance over time so that the proportion of Se(0) to selenoamino acids (62%:38%, respectively) was similar to all the other growth conditions by day 20. The rapid formation of these different Se compounds upon Se(IV) exposure, as well as the overall consistency with which they were formed under most experimental conditions through the various growth stages, suggests that Se(IV) detoxification mechanisms were either upregulated immediately upon exposure or they occurred independently of Se presence. Studies to decipher the mechanisms of Se biotransformation are warranted and should consider the variety of Se bioproducts formed under the different growth conditions (e.g., those in which the Se compounds are consistently produced versus those in which the products change over time or growth stage).

3.2.2. Microscopic Examination of Biogenic Se(0). This study sought to examine mycogenic Se(0) morphology, structure, and cellular location to see if and how SeNPs evolved through different fungal growth stages and over time. Microscopic examination of hyphal cross sections revealed that

https://doi.org/10.1021/acsearthspacechem.2c00288
ACS Earth Space Chem. 2023, 7, 960−971

all of the Se(0) identified by EXAFS existed as amorphous SeNPs (Figure 5 and Figures S5a−c), regardless of fungal species, Se concentration, or fungal growth stage. Energy Dispersive Spectroscopy (EDS) confirmed that the electron-dense nanoparticles were rich in Se, as opposed to background intracellular material which did not contain detectable Se (Figure S5d). This was expected based on previous studies of fungal and bacterial SeNP characterization.[2,29,32,45,69−71] The biggest differences observed in SeNPs from the two fungal isolates were the size and morphology. Specifically, *A. alternata* produced aggregates of very small SeNPs as early as day 5, particularly outside the cell (Figures 5a,b). The individual nanoparticles were ∼10−20 nm and aggregates ranged in size and shape but were generally no larger than ∼500 nm in diameter (Figure 5b). The SeNPs typically aggregated into clusters, but sometimes joined together extracellularly to form filamentous "nanowires" or "chains" that resembled microbial cells except for their extremely small size and consistent Se presence based on EDS. These nanowires were similar to those observed by Se reduction with cytochrome c_3.[72] At each time point, larger (∼100 nm) individual intracellular and extracellular nanoparticles were also sporadically observed. Neither individual SeNPs nor SeNP aggregates appeared to grow larger with time, but the total amount generally increased throughout the experiment as expected with increased solid-associated Se concentrations. In contrast, the SeNPs produced by *P. sporulosa* were generally much larger than the particles produced by *A. alternata* (∼200−500 nm diameter), nonaggregated (i.e., individual), and spherical (Figures 5c,d). It could not be discerned if SeNP density increased over time. SeNP aggregates were only occasionally observed in the *P. sporulosa* cultures, though there was no apparent trend relating their occurrence to specific experimental conditions or growth stages. It is possible that Ostwald's ripening mechanisms occurred to form some of the larger *P. sporulosa* nanoparticles,[73,74] but NPs were never observed with diameters greater than ∼500 nm and there were not any discernible differences in average size of SeNPs at day 5 compared to day 20.

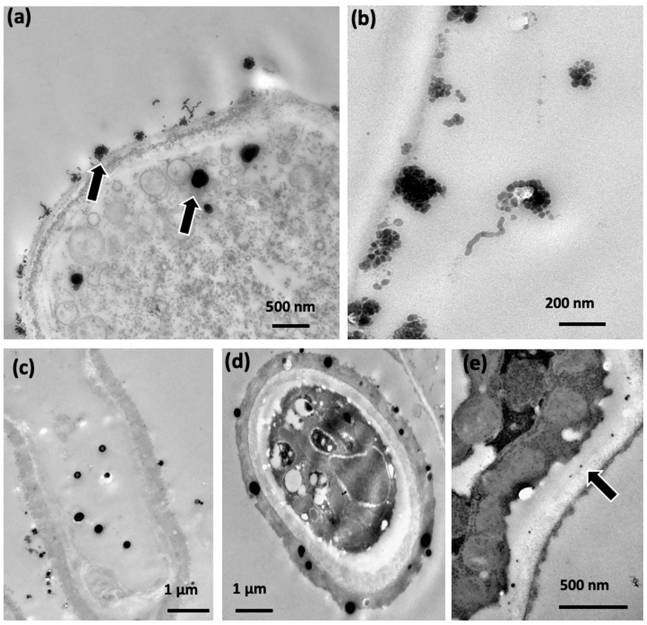

Figure 5. Transmission electron microscopy (TEM) images of cross sections through fungal hyphae of *A. alternata* (a, b) and *P. sporulosa* (c, d, e) showing electron dense SeNPs. (a) Black arrows highlight extracellular and intracellular SeNPs. (b) Extracellular aggregates and filaments of small SeNPs were characteristic for *A. alternata*. (c) Spherical nature of larger, individual SeNPs produced by *P. sporulosa*. (d) SeNPs embedded in the cell wall and (e) aligned along the interior of the cell membrane (black arrow) suggest that these particles could be expelled outside the cell.

For both fungi, SeNPs were strongly associated with the biomass either within the cytoplasm, along the cell membrane interior, embedded within the cell wall, and outside the hyphal cell (Figure 5). Extracellular SeNPs were commonly in close association with the cell wall, even after a somewhat disruptive TEM preparation protocol, which suggests that these NPs were bound by extracellular polymeric substances (EPS) or some other organic compounds. It is feasible that all the SeNPs were formed intracellularly and a fraction were expelled through vesicles or other means outside the cell. Indeed, TEM images of hyphal cross sections show nanoparticles both lining the interior of the cell membrane (Figure 5e) or embedded within the thick β-glucans layer of the cell wall (Figure 5d), potentially en route to cellular expulsion. While it may seem unexpected for large particles to be transported across the fungal cell wall, previous work showed that 60−80 nm liposome vesicles were able to pass through the fungal cell membrane completely intact.[75] A diversity of Ascomycete fungi have been shown to export intracellular material through transmembrane vesicular transport[76] and some yeasts have been observed to expel SeNPs through this pathway.[77] TEM analysis of the fungi in this study showed evidence of potential vesicles (Figure 5a, left of intracellular SeNP with black arrow), but it was not definitive that the SeNPs were encapsulated by these vesicles. Direct extracellular SeNP synthesis pathways could have also been active, as highly reducing thiols and other enzymes produced by the fungus could have reduced the Se(IV) to Se(0).[74,78] The abundance of very small, extracellular SeNPs by *A. alternata* may suggest this formation pathway, although this hypothesis is quite speculative.

Although individual Se(0) biominerals could not be tracked over time, examination of numerous fungal cells at different spatial scales were performed to give confidence that these particles are stable over time. The amorphous nature of the SeNPs, their size ranges, and cellular locations appeared consistent from day 5 through 32. Previous studies observed that EPS and specific proteins are associated with biogenic SeNPs.[71,79,80] These protein coatings help stabilize the SeNPs,[81] minimizing physicochemical alteration or further Se reduction or oxidation by biotic or abiotic processes. It has also been suggested that these proteins and other organic compounds may help control the size and morphology of the SeNPs.[72,82] In the study by Wang et al.,[73] they hypothesized that the proteins prevented aggregation of the SeNPs. This could indicate that *A. alternata* produced SeNPs with either minimal or no proteins, or a specific organic compound that strongly inhibited particle size growth (e.g., Ostwald's ripening) but promoted aggregation. More work is necessary on the SeNPs formed by each organism to understand the causes for these different particle sizes and morphologies. It cannot be entirely ruled out, however, that the SeNPs are rapidly being formed and reoxidized or reduced to form other Se bioproducts. The lack of Se(IV) or Se(VI) detected with the fungal biomass by EXAFS analysis throughout the course of the experiments indicates that

https://doi.org/10.1021/acsearthspacechem.2c00288
ACS Earth Space Chem. 2023, 7, 960−971

Se(0) reoxidation is unlikely (Figure 4). Se(0) reduction to Se(-II), and subsequent methylation or selenoamino acid formation is also a potential transformation pathway.[25,32] However, the stable relative proportions of the different Se species throughout most experiments suggests that the Se(0) is likely stable after formation, except for the 0.1 mM Se experiment with *P. sporulosa*. The relative increase in organoselenium compounds and concomitant Se(0) decrease during exponential growth of *P. sporulosa* may suggest that these initial SeNPs were not stable for the first ∼20 days. Separation of the SeNPs and interrogation using other analytical techniques that can assess the organic components in a more detailed fashion should shed light on the causes of SeNP variation observed in this study.

3.2.3. Applications of Fungal Se(IV) Reduction and Se Bioproducts. The fast removal of toxic levels of Se(IV) from soils and waters by fungi through reduction to either volatile methylated selenides (e.g., DMSe) or SeNPs has important implications for the remediation of polluted environments.[83] There are different factors to consider for effective Se(IV) removal such as the environmental conditions present as well as fungal physiology, project cost, policies in place, and more. For example, Se transformation to less toxic, volatile forms might be preferred if large swaths of Se-contaminated soils can be remediated using these fungal amendments.[62,84] *A. alternata* proved highly effective in volatilizing Se in this study and others,[9] but further research on this specific strain is necessary before implementing soil amendments as some Alternaria strains are known plant pathogens.[85,86] In a contained or constructed environment such as those treating Se-contaminated industrial wastewater, this species could be highly effective in removing hazardous levels of Se(IV). Other fungal Ascomycete species studied previously[2,28] were also highly effective at volatilizing Se(IV) and Se(VI) with minimal production of solid-phase Se, which might be preferred in some bioremediation applications. If Se volatilization and release to the atmosphere is not preferred, however, *A. alternata* was highly effective at immobilizing Se by quickly producing SeNPs and selenoproteins at all growth stages and could be an excellent candidate for this bioremediation approach. Further, the biomass or nanoparticles could be harvested via filtration for Se removal and possible reuse,[84] thus building a circular economy for these natural and sustainable bioremediation products. The SeNPs and proteins were stable over time in the present experimental conditions, but more work will be necessary to determine their stability over time in more complex environments such as soils containing potential oxidants.[32,87−89] Additionally, factors such as carbon source and concentration can influence the proportion of the various Se transformation products.[45] In a more controlled bioreactor, optimization of conditions that promote SeNP formation would benefit from greater understanding of the biological mechanisms that specifically promote Se(IV) reduction to Se(0) compared to other Se transformation pathways and products.

In contrast to issues surrounding Se-polluted environments, some soils are severely depleted in selenium and volatilization could be detrimental. Since plants serve as the primary Se dietary source to all animals,[90,91] Se concentrations and speciation (i.e., bioavailability) in soils are the primary factor controlling dietary sufficiency in a region.[92] It is estimated that one in seven people currently have Se deficient diets, and changes in climate are expected to exacerbate that problem through decreased Se soil concentrations.[93] While Se volatilization naturally occurs in soils by plants and microorganisms,[4,94] processes that further stimulate Se loss, particularly in agricultural areas, could be highly detrimental to livestock and human health. While Se volatilization was not substantial at higher Se concentrations, relatively large amounts of Se were volatilized (∼39% by *A. alternata* and ∼17% by *P. sporulosa*) after just 1 month of growth under the moderate Se concentrations used in this study. These fungi might be capable of mediating further Se removal from soils at very low Se levels, despite their ability to immobilize some of the Se as selenoproteins and Se(0). Indeed, the study by Karlson and Frankenberger[62] found that Se volatilization rates by fungal amended soils were fastest at the lowest Se(IV) concentrations. Further investigations into fungal volatilization mechanisms and pathways for Se(IV) and Se(VI), as well as the stability of immobilized Se forms, are necessary for applied agricultural purposes such as applying fungal or chemical amendments to stimulate plant growth that might alter the fungal physiology.

The fungal bioproduction of SeNPs and selenoamino acids upon exposure to Se(IV) also has great potential for the medical field and other biotechnology sectors that use SeNPs for their antimicrobial and antioxidant properties.[15,66,95] As their effectiveness is dependent on parameters such as NP size,[66,96] the causes and control over SeNP morphology and size produced by fungi in this study will be important to resolve for applications such as this. SeNPs with various physicochemical parameters (e.g., crystallinity, composition, surface area, etc.) and photoelectric and semiconducting properties are also being developed for use in electronics and optics[15,97] or as nanobiosensors for the detection of hydrogen peroxide,[73] although these typically are not the amorphous SeNPs generated by fungi and would require post-treatment or modification before application. Organic Se forms such as selenoamino acids and selenoproteins are commonly used as nutritional supplements for human and other animal diets,[98] although some forms such as selenomethionine have also been shown to be toxic.[68] It is not clear if interactions between these various organic and inorganic Se bioproducts enhance or detract from their potential application. Future research would greatly benefit from examining these complex biomaterials and interactions over time and ways to optimize the biosynthesis of these different Se bioproducts.

■ CONCLUSIONS

The results from this study emphasize the complexity of factors (e.g., fungal species, fungal growth stage, Se form and concentration) that influence fungal Se(IV) removal and transformation. While several Se biotransformation products were generated in these experiments, the general consistency with which these bioproducts were formed throughout fungal growth (especially the relative proportions of Se(0) and organo-Se compounds) suggests that these processes are also consistent, predictable, and controllable in natural and constructed environments. Effective fungal Se(IV) removal and Se bioproduct synthesis therefore represents a viable, greener approach to biotechnologies such as bioremediation and biomedicine. If specific Se products are desired, identifying the fungal Se(IV) reduction mechanisms that lead to these specific products as well as further investigations of Se bioproduct interactions with other biologically or environmentally relevant metal(loids) will be valuable. Further

https://doi.org/10.1021/acsearthspacechem.2c00288
ACS Earth Space Chem. 2023, 7, 960−971

examination of fungal Se(VI) reduction pathways and bioproduct formation, not examined in this study, will also prove valuable for understanding the environmental impact and application of fungal Se transformations. Continued research that employs genomic approaches and other analytical methods will facilitate these biotechnological applications as well as provide a more robust assessment of the role and impact of fungi in the biogeochemical cycling and distribution of Se in the environment.

■ ASSOCIATED CONTENT

Data Availability Statement

All data generated from this study are freely available on Figshare at the following DOIs: Table S1—Biomass weights: dx.doi.org/10.6084/m9.figshare.20666115. Table S2—Aqueous Phase Se(IV): dx.doi.org/10.6084/m9.figshare.20666166. Table S3—Mass balance: dx.doi.org/10.6084/m9.figshare.20666223. Table S4—Solid-associated Se: dx.doi.org/10.6084/m9.figshare.20666313. Table S5—XAS: dx.doi.org/10.6084/m9.figshare.20666262.

Supporting Information

The Supporting Information is available free of charge at https://pubs.acs.org/doi/10.1021/acsearthspacechem.2c00288.

Net dry biomass for abiotic biomass-free and killed-biomass control experiments (Figure S1); aqueous Se(IV) concentration remaining in solution over time for killed biomass control experiments (Figure S2); solid- or biomass-associated Se concentrations (Figure S3); Se K-edge EXAFS spectra (Figure S4); Transmission electron microscopy of cross sections through fungal hyphae, electron diffraction images of SeNPs, EDS spectra of SeNPs and intracellular matrix (Figure S5) (PDF)

■ AUTHOR INFORMATION

Corresponding Author

Cara M. Santelli − *Department of Earth and Environmental Sciences, Minneapolis, Minnesota 55455, United States; BioTechnology Institute, University of Minnesota, Saint Paul, Minnesota 55108, United States;* orcid.org/0000-0001-8617-0008; Email: santelli@umn.edu

Authors

Mary C. Sabuda − *Department of Earth and Environmental Sciences, Minneapolis, Minnesota 55455, United States; BioTechnology Institute, University of Minnesota, Saint Paul, Minnesota 55108, United States;* Present Address: American Chemical Society, 1155 16th Street NW, Washington, DC 20036, United States; orcid.org/0000-0002-2503-9943

Carla E. Rosenfeld − *Section of Minerals and Earth Sciences, Carnegie Museum of Natural History, Pittsburgh, Pennsylvania 15213, United States;* orcid.org/0000-0002-5870-5906

Complete contact information is available at: https://pubs.acs.org/10.1021/acsearthspacechem.2c00288

Author Contributions

The manuscript was written through contributions of all authors. CMS, MCS, and CER created and designed the study. MCS and CER performed laboratory experiments and conducted sample and data analysis. MCS, CER, and CMS created the figures and tables, and CMS wrote the manuscript with input, critical discussion, and edits from MCS and CER. All authors have seen and approved the final version of this manuscript.

Notes

The authors declare no competing financial interest.

■ ACKNOWLEDGMENTS

Research was supported by a NSF CAREER award to CMS (NSF #1749727) and a University of Minnesota Informatics Institute - MnDRIVE Fellowship to MCS. The funders had no role in project design, implementation, or analysis. Parts of this work were carried out in the Characterization Facility, University of Minnesota, which receives partial support from NSF through the MRSEC program. We thank Fang Zhou and Bob Hafner for assistance and training with TEM sample preparation and imaging. We thank Jason Myers for help with TEM analysis. This research used resources of the Advanced Photon Source, a U.S. Department of Energy (DOE) Office of Science User Facility operated for the DOE Office of Science by Argonne National Laboratory under Contract No. DE-AC02-06CH11357. We thank Ben Reinhart for his help with XAS data collection, and Christine Hitomi and Josh Torgeson for experimental assistance.

■ REFERENCES

(1) Nancharaiah, Y. V.; Lens, P. N. Ecology and biotechnology of selenium-respiring bacteria. *Microbiology and molecular biology reviews: MMBR* **2015**, *79* (1), 61−80.

(2) Rosenfeld, C. E.; Kenyon, J. A.; James, B. R.; Santelli, C. M. Selenium (IV,VI) reduction and tolerance by fungi in an oxic environment. *Geobiology* **2017**, *15* (3), 441−452.

(3) Gharieb, M. M.; Wilkinson, S. C.; Gadd, G. M. Reduction of Selenium Oxyanions by Unicellular, Polymorphic and Filamentous Fungi - Cellular Location of Reduced Selenium and Implications for Tolerance. *Journal of Industrial Microbiology* **1995**, *14* (3−4), 300−311.

(4) Wells, M.; Stolz, J. F. Microbial selenium metabolism: a brief history, biogeochemistry and ecophysiology. *FEMS Microbiol. Ecol* **2020**, DOI: 10.1093/femsec/fiaa209.

(5) Yee, N.; Ma, J.; Dalia, A.; Boonfueng, T.; Kobayashi, D. Y. Se(VI) reduction and the precipitation of Se(0) by the facultative bacterium *Enterobacter cloacae SLD1a-1* are regulated by FNR. *Appl. Environ. Microbiol.* **2007**, *73* (6), 1914−20.

(6) Stolz, J. F.; Basu, P.; Santini, J. M.; Oremland, R. S. Arsenic and selenium in microbial metabolism. *Annual review of microbiology* **2006**, *60*, 107−30.

(7) Kessi, J.; Hanselmann, K. W. Similarities between the abiotic reduction of selenite with glutathione and the dissimilatory reaction mediated by *Rhodospirillum rubrum* and *Escherichia coli*. *J. Biol. Chem.* **2004**, *279* (49), 50662−9.

(8) Cooke, T. D.; Bruland, K. W. Aquatic chemistry of selenium: evidence of biomethylation. *Environ. Sci. Technol.* **1987**, *21* (12), 1214−1219.

(9) Thompson-Eagle, E. T.; Frankenberger, W. T.; Karlson, U. Volatilization of Selenium by *Alternaria alternata*. *Appl. Environ. Microbiol.* **1989**, *55* (6), 1406−13.

(10) Xu, X. M.; Carlson, B. A.; Zhang, Y.; Mix, H.; Kryukov, G. V.; Glass, R. S.; Berry, M. J.; Gladyshev, V. N.; Hatfield, D. L. New developments in selenium biochemistry: selenocysteine biosynthesis in eukaryotes and archaea. *Biol. Trace Elem Res.* **2007**, *119* (3), 234−41.

(11) Ranjard, L.; Nazaret, S.; Cournoyer, B. Freshwater bacteria can methylate selenium through the thiopurine methyltransferase pathway. *Appl. Environ. Microbiol.* **2003**, *69* (7), 3784−90.

(12) Allmang, C.; Wurth, L.; Krol, A. The selenium to selenoprotein pathway in eukaryotes: more molecular partners than anticipated. *Biochimica et biophysica acta* **2009**, *1790* (11), 1415−23.
(13) Winkel, L. H.; Vriens, B.; Jones, G. D.; Schneider, L. S.; Pilon-Smits, E.; Banuelos, G. S. Selenium cycling across soil-plant-atmosphere interfaces: a critical review. *Nutrients* **2015**, *7* (6), 4199−239.
(14) Benko, I.; Nagy, G.; Tanczos, B.; Ungvari, E.; Sztrik, A.; Eszenyi, P.; Prokisch, J.; Banfalvi, G. Subacute toxicity of nano-selenium compared to other selenium species in mice. *Environ. Toxicol. Chem.* **2012**, *31* (12), 2812−20.
(15) Wadhwani, S. A.; Shedbalkar, U. U.; Singh, R.; Chopade, B. A. Biogenic selenium nanoparticles: current status and future prospects. *Appl. Microbiol. Biotechnol.* **2016**, *100* (6), 2555−66.
(16) Shi, X. D.; Tian, Y. Q.; Wu, J. L.; Wang, S. Y. Synthesis, characterization, and biological activity of selenium nanoparticles conjugated with polysaccharides. *Crit Rev. Food Sci. Nutr* **2021**, *61* (13), 2225−2236.
(17) Letavayova, L.; Vlasakova, D.; Spallholz, J. E.; Brozmanova, J.; Chovanec, M. Toxicity and mutagenicity of selenium compounds in *Saccharomyces cerevisiae*. *Mutat. Res.* **2008**, *638* (1−2), 1−10.
(18) Obermeyer, B. D.; Palmer, I. S.; Olson, O. E.; Halverson, A. W. Toxicity of trimethylselenonium chloride in the rat with and without arsenite. *Toxicol. Appl. Pharmacol.* **1971**, *20* (2), 135−146.
(19) Ganther, H. E. Selenotrisulfides. Formation by the reaction of thiols with selenious acid. *Biochemistry* **1968**, *7* (8), 2898−905.
(20) Steinbrenner, H.; Sies, H. Protection against reactive oxygen species by selenoproteins. *Biochimica et biophysica acta* **2009**, *1790* (11), 1478−85.
(21) Pócsi, I.; Prade, R. A.; Penninckx, M. J. Glutathione, Altruistic Metabolite in Fungi. *Adv. Microb. Physiol.* **2004**, *49*, 1−76.
(22) Wangeline, A. L.; Valdez, J. R.; Lindblom, S. D.; Bowling, K. L.; Reeves, F. B.; Pilon-Smits, E. A. Characterization of rhizosphere fungi from selenium hyperaccumulator and nonhyperaccumulator plants along the eastern Rocky Mountain Front Range. *Am. J. Bot* **2011**, *98* (7), 1139−47.
(23) Sabuda, M. C.; Rosenfeld, C. E.; DeJournett, T. D.; Schroeder, K.; Wuolo-Journey, K.; Santelli, C. M. Fungal Bioremediation of Selenium-Contaminated Industrial and Municipal Wastewaters. *Front. Microbiol.* **2020**, DOI: 10.3389/fmicb.2020.02105.
(24) Frankenberger, W. T.; Karlson, U. Volatilization of selenium from a dewatered seleniferous sediment: a field study. *Journal of Industrial Microbiology* **1995**, *14*, 226−232.
(25) Lenz, M.; Lens, P. N. The essential toxin: the changing perception of selenium in environmental sciences. *Science of the total environment* **2009**, *407* (12), 3620−33.
(26) Kaur, T.; Vashisht, A.; Prakash, N. T.; Reddy, M. S. Role of Selenium-Tolerant Fungi on Plant Growth Promotion and Selenium Accumulation of Maize Plants Grown in Seleniferous Soils. *Water, Air, Soil Pollution* **2022**, DOI: 10.1007/s11270-021-05490-9.
(27) Rosenfeld, C. E.; James, B. R.; Santelli, C. M. Persistent Bacterial and Fungal Community Shifts Exhibited in Selenium-Contaminated Reclaimed Mine Soils. *Appl. Environ. Microbiol.* **2018**, DOI: 10.1128/AEM.01394-18.
(28) Brady, J. M.; Tobin, J. M.; Gadd, G. M. Volatilization of selenite in aqueous medium by a Penicillium species. *Mycological Research* **1996**, *100* (8), 955−961.
(29) Zhang, H.; Zhou, H.; Bai, J.; Li, Y.; Yang, J.; Ma, Q.; Qu, Y. Biosynthesis of selenium nanoparticles mediated by fungus *Mariannaea* sp. HJ and their characterization. *Colloids Surf., A* **2019**, *571*, 9−16.
(30) Ruocco, M. H. W.; Chan, C. S.; Hanson, T. E.; Church, T. M. Characterization and Distribution of Selenite Reduction Products in Cultures of the Marine Yeast *Rhodotorula mucilaginosa-13B*. *Geomicrobiology Journal* **2014**, *31* (9), 769−778.
(31) Liang, X.; Perez, M. A. M.; Nwoko, K. C.; Egbers, P.; Feldmann, J.; Csetenyi, L.; Gadd, G. M. Fungal formation of selenium and tellurium nanoparticles. *Appl. Microbiol. Biotechnol.* **2019**, *103* (17), 7241−7259.
(32) Rosenfeld, C. E.; Sabuda, M. C.; Hinkle, M. A. G.; James, B. R.; Santelli, C. M. A Fungal-Mediated Cryptic Selenium Cycle Linked to Manganese Biogeochemistry. *Environ. Sci. Technol.* **2020**, *54* (6), 3570−3580.
(33) Bierla, K.; Szpunar, J.; Yiannikouris, A.; Lobinski, R. Comprehensive speciation of selenium in selenium-rich yeast. *TrAC Trends in Analytical Chemistry* **2012**, *41*, 122−132.
(34) Gilbert-Lopez, B.; Dernovics, M.; Moreno-Gonzalez, D.; Molina-Diaz, A.; Garcia-Reyes, J. F. Detection of over 100 selenium metabolites in selenized yeast by liquid chromatography electrospray time-of-flight mass spectrometry. *J. Chromatogr B Analyt Technol. Biomed Life Sci.* **2017**, *1060*, 84−90.
(35) Mariotti, M.; Santesmasses, D.; Capella-Gutierrez, S.; Mateo, A.; Arnan, C.; Johnson, R.; D'Aniello, S.; Yim, S. H.; Gladyshev, V. N.; Serras, F.; Corominas, M.; Gabaldon, T.; Guigo, R. Evolution of selenophosphate synthetases: emergence and relocation of function through independent duplications and recurrent subfunctionalization. *Genome Res.* **2015**, *25* (9), 1256−67.
(36) Lobanov, A. V.; Hatfield, D. L.; Gladyshev, V. N. Eukaryotic selenoproteins and selenoproteomes. *Biochimica et biophysica acta* **2009**, *1790* (11), 1424−8.
(37) Mariotti, M.; Salinas, G.; Gabaldon, T.; Gladyshev, V. N. Utilization of selenocysteine in early-branching fungal phyla. *Nat. Microbiol* **2019**, *4*, 759.
(38) Daniels, L. A. Selenium metabolism and bioavailability. *Biol. Trace Elem Res.* **1996**, *54* (3), 185−99.
(39) Rosenfeld, I. Biosynthesis of seleno-compounds from inorganic selenium by sheep. *Proc. Soc. Exp Biol. Med.* **1962**, *111*, 670−3.
(40) Iwaoka, M.; Ooka, R.; Nakazato, T.; Yoshida, S.; Oishi, S. Synthesis of selenocysteine and selenomethionine derivatives from sulfur-containing amino acids. *Chem. Biodivers* **2008**, *5* (3), 359−74.
(41) Vrabl, P.; Schinagl, C. W.; Artmann, D. J.; Heiss, B.; Burgstaller, W. Fungal Growth in Batch Culture - What We Could Benefit If We Start Looking Closer. *Front Microbiol* **2019**, *10*, 2391.
(42) Smedsgaard, J.; Nielsen, J. Metabolite profiling of fungi and yeast: from phenotype to metabolome by MS and informatics. *J. Exp Bot* **2005**, *56* (410), 273−86.
(43) Kluger, B.; Lehner, S.; Schuhmacher, R. Metabolomics and Secondary Metabolite Profiling of Filamentous Fungi. In *Biosynthesis and Molecular Genetics of Fungal Secondary Metabolites*; Springer: New York, NY, 2015; Vol. 2, pp 81−101. DOI: 10.1007/978-1-4939-2531-5_6.
(44) Zeiner, C. A.; Purvine, S. O.; Zink, E.; Wu, S.; Paša-Tolić, L.; Chaput, D. L.; Santelli, C. M.; Hansel, C. M. Mechanisms of Manganese(II) Oxidation by Filamentous Ascomycete Fungi Vary With Species and Time as a Function of Secretome Composition. *Front. Microbiol.* **2021**, DOI: 10.3389/fmicb.2021.610497.
(45) Sabuda, M. C.; Mejia, J.; Wedal, M.; Kuester, B.; Xu, T.; Santelli, C. M. The effect of organic carbon form and concentration on fungal selenite reduction. *Appl. Geochem.* **2022**, *136*, 105163.
(46) Santelli, C. M.; Pfister, D.; Lazarus, D.; Sun, L.; Burgos, W. D.; Hansel, C. M. Diverse fungal and bacterial communities promote Mn(II)-oxidation and remediation of coal mine drainage in passive treatment systems. *Appl. Environ. Microbiol.* **2010**, *76* (14), 4871−4875.
(47) Santelli, C. M.; Chaput, D. L.; Hansel, C. M. Microbial Communities Promoting Mn(II) Oxidation in Ashumet Pond, a Historically Polluted Freshwater Pond Undergoing Remediation. *Geomicrobiol. J.* **2014**, *31* (7), 605−616.
(48) Miyata, N.; Tani, Y.; Iwahori, K.; Soma, M. Enzymatic formation of manganese oxides by an *Acremonium*-like hyphomycete fungus, strain KR 21−2. *FEMS Microbiol. Ecol.* **2004**, *47* (1), 101−109.
(49) Santelli, C. M.; Webb, S. M.; Dohnalkova, A. C.; Hansel, C. M. Diversity of Mn oxides produced by Mn(II)-oxidizing fungi. *Geochim. Cosmochim. Acta* **2011**, *75* (10), 2762−2776.
(50) Ravel, B.; Newville, M. ATHENA, ARTEMIS, HEPHAESTUS: data analysis for X-ray absorption spectroscopy using IFEFFIT. *J. Synchrotron Radiat* **2005**, *12* (4), 537−541.

(51) Newville, M. IFEFFIT: interactive XAFS analysis and FEFF fitting. *J. Synchrotron Radiat* **2001**, *8* (2), 322−324.
(52) Nie, T.; Wu, H.; Wong, K.-H.; Chen, T. Facile synthesis of highly uniform selenium nanoparticles using glucose as the reductant and surface decorator to induce cancer cell apoptosis. *J. Mater. Chem. B* **2016**, *4* (13), 2351−2358.
(53) Islam, M. R.; Tudryn, G.; Bucinell, R.; Schadler, L.; Picu, R. C. Morphology and mechanics of fungal mycelium. *Sci. Rep* **2017**, *7* (1), 13070.
(54) Aynsley, M.; Ward, A. C.; Wright, A. R. A mathematical model for the growth of mycelial fungi in submerged culture. *Biotechnol. Bioeng.* **1990**, *35* (8), 820−30.
(55) Lundy, S. D.; payne, R. J.; Giles, K. R.; Garrill, A. Heavy metals have different effects on mycelial morphology of *Achlya bisexualis* as determined by fractal geometry. *FEMS Microbiol. Lett.* **2001**, *201*, 259−263.
(56) Urík, M.; Bujdoš, M.; Gardošová, K.; Littera, P.; Matúš, P. Selenite Distribution in Multicomponent System Consisting of Filamentous Fungus, Humic Acids, Bentonite, and Ferric Oxyhydroxides. *Water, Air, Soil Pollution* **2018**, DOI: 10.1007/s11270-018-3719-z.
(57) Spallholz, J. E. On the nature of selenium toxicity and carcinostatic activity. *Free Radical Biol. Med.* **1994**, *17* (1), 45−64.
(58) Painter, E. P. The Chemistry and Toxicity of Selenium Compounds, with Special Reference to the Selenium Problem. *Chem. Rev.* **1941**, *28* (2), 179−213.
(59) Zhang, J. S.; Gao, X. Y.; Zhang, L. D.; Bao, Y. P. Biological effects of a nano red elemental selenium. *Biofactors* **2001**, *15* (1), 27−38.
(60) Fernández-Martínez, A.; Charlet, L. Selenium environmental cycling and bioavailability: a structural chemist point of view. *Reviews in Environmental Science and Bio/Technology* **2009**, *8* (1), 81−110.
(61) Chasteen, T. G.; Bentley, R. Biomethylation of selenium and tellurium: microorganisms and plants. *Chem. Rev.* **2003**, *103* (1), 1−25.
(62) Karlson, U.; Frankenberger, W. T. Accelerated rates of selenium volatilization from California soils. *Soil Sci. Soc. Am. J.* **1989**, *53*, 749−753.
(63) Fleming, R. W.; Alexander, M. Dimethylselenide and dimethyltelluride formation by a strain of Penicillium. *Appl. Microbiol.* **1972**, *24* (3), 424−9.
(64) Doran, J. W. Microorganisms and the Biological Cycling of Selenium. *In Advances in Microbial Ecology* **1982**, *6*, 1−32.
(65) Jain, R.; Matassa, S.; Singh, S.; van Hullebusch, E. D.; Esposito, G.; Lens, P. N. Reduction of selenite to elemental selenium nanoparticles by activated sludge. *Environmental science and pollution research international* **2016**, *23*, 1193.
(66) Torres, S. K.; Campos, V. L.; León, C. G.; Rodríguez-Llamazares, S. M.; Rojas, S. M.; González, M.; Smith, C.; Mondaca, M. A. Biosynthesis of selenium nanoparticles by *Pantoea agglomerans* and their antioxidant activity. *J. Nanopart. Res.* **2012**, DOI: 10.1007/s11051-012-1236-3.
(67) Bird, S. M.; Uden, P. C.; Tyson, J. F.; Block, E.; Denoyer, E. Speciation of Selenoamino Acids and Organoselenium Compounds in Selenium-enriched Yeast Using High-performance Liquid Chromatography−Inductively Coupled Plasma Mass Spectrometry. *J. Anal. At. Spectrom.* **1997**, *12* (7), 785−788.
(68) Lazard, M.; Dauplais, M.; Blanquet, S.; Plateau, P. Trans-sulfuration Pathway Seleno-amino Acids Are Mediators of Selenomethionine Toxicity in *Saccharomyces cerevisiae*. *J. Biol. Chem.* **2015**, *290* (17), 10741−50.
(69) Fakra, S. C.; Luef, B.; Castelle, C. J.; Mullin, S. W.; Williams, K. H.; Marcus, M. A.; Schichnes, D.; Banfield, J. F. Correlative cryogenic spectro-microscopy to investigate Selenium bioreduction products. *Environ. Sci. Technol.* **2018**, *52*, 503.
(70) Oremland, R. S.; Herbel, M. J.; Blum, J. S.; Langley, S.; Beveridge, T. J.; Ajayan, P. M.; Sutto, T.; Ellis, A. V.; Curran, S. Structural and spectral features of selenium nanospheres produced by Se-respiring bacteria. *Appl. Environ. Microbiol.* **2004**, *70* (1), 52−60.
(71) Lenz, M.; Kolvenbach, B.; Gygax, B.; Moes, S.; Corvini, P. F. Shedding light on selenium biomineralization: proteins associated with bionanominerals. *Appl. Environ. Microbiol.* **2011**, *77* (13), 4676−80.
(72) Abdelouas, A.; Gong, W. L.; Lutze, W.; Shelnutt, J. A.; Franco, R.; Moura, I. Using Cytochrome c3 To Make Selenium Nanowires. *Chem. Mater.* **2000**, *12* (6), 1510−1512.
(73) Wang, T.; Yang, L.; Zhang, B.; Liu, J. Extracellular biosynthesis and transformation of selenium nanoparticles and application in H2O2 biosensor. *Colloids Surf. B Biointerfaces* **2010**, *80* (1), 94−102.
(74) Lampis, S.; Zonaro, E.; Bertolini, C.; Bernardi, P.; Butler, C. S.; Vallini, G. Delayed formation of zero-valent selenium nanoparticles by *Bacillus mycoides* SeITE01 as a consequence of selenite reduction under aerobic conditions. *Microb Cell Fact* **2014**, *13* (1), 35.
(75) Walker, L.; Sood, P.; Lenardon, M. D.; Milne, G.; Olson, J.; Jensen, G.; Wolf, J.; Casadevall, A.; Adler-Moore, J.; Gow, N. A. R. The Viscoelastic Properties of the Fungal Cell Wall Allow Traffic of AmBisome as Intact Liposome Vesicles. *mBio* **2018**, DOI: 10.1128/mBio.02383-17.
(76) Casadevall, A.; Nosanchuk, J. D.; Williamson, P.; Rodrigues, M. L. Vesicular transport across the fungal cell wall. *Trends Microbiol* **2009**, *17* (4), 158−62.
(77) Zhang, L.; Li, D.; Gao, P. Expulsion of selenium/protein nanoparticles through vesicle-like structures by *Saccharomyces cerevisiae* under microaerophilic environment. *World J. Microbiol. Biotechnol.* **2012**, *28* (12), 3381−6.
(78) Dwivedi, S.; Alkhedhairy, A. A.; Ahamed, M.; Musarrat, J. Biomimetic synthesis of selenium nanospheres by bacterial strain JS-11 and its role as a biosensor for nanotoxicity assessment: a novel se-bioassay. *PLoS One* **2013**, *8* (3), No. e57404.
(79) Tugarova, A. V.; Kamnev, A. A. Proteins in microbial synthesis of selenium nanoparticles. *Talanta* **2017**, *174*, 539−547.
(80) Xu, D.; Yang, L.; Wang, Y.; Wang, G.; Rensing, C.; Zheng, S. Proteins enriched in charged amino acids control the formation and stabilization of selenium nanoparticles in *Comamonas testosteroni* S44. *Sci. Rep* **2018**, *8* (1), 4766.
(81) Debieux, C. M.; Dridge, E. J.; Mueller, C. M.; Splatt, P.; Paszkiewicz, K.; Knight, I.; Florance, H.; Love, J.; Titball, R. W.; Lewis, R. J.; Richardson, D. J.; Butler, C. S. A bacterial process for selenium nanosphere assembly. *Proc. Natl. Acad. Sci. U. S. A.* **2011**, *108* (33), 13480−5.
(82) Dobias, J.; Suvorova, E. I.; Bernier-Latmani, R. Role of proteins in controlling selenium nanoparticle size. *Nanotechnology* **2011**, *22* (19), No. 195605.
(83) Nancharaiah, Y. V.; Lens, P. N. Selenium biomineralization for biotechnological applications. *Trends Biotechnol* **2015**, *33* (6), 323−30.
(84) Frankenberger, W. T., Jr.; Arshad, M. Bioremediation of selenium-contaminated sediments and water. *Biofactors* **2001**, *14* (1−4), 241−54.
(85) Tsuge, T.; Harimoto, Y.; Akimitsu, K.; Ohtani, K.; Kodama, M.; Akagi, Y.; Egusa, M.; Yamamoto, M.; Otani, H. Host-selective toxins produced by the plant pathogenic fungus *Alternaria alternata*. *FEMS Microbiol Rev.* **2013**, *37* (1), 44−66.
(86) DeMers, M. *Alternaria alternata* as endophyte and pathogen. *Microbiology* **2022**, DOI: 10.1099/mic.0.001153.
(87) Wang, X.; Zhang, D.; Qian, H.; Liang, Y.; Pan, X.; Gadd, G. M. Interactions between biogenic selenium nanoparticles and goethite colloids and consequence for remediation of elemental mercury contaminated groundwater. *Science of the total environment* **2018**, *613−614*, 672−678.
(88) Buchs, B.; Evangelou, M. W.; Winkel, L. H.; Lenz, M. Colloidal properties of nanoparticular biogenic selenium govern environmental fate and bioremediation effectiveness. *Environ. Sci. Technol.* **2013**, *47* (5), 2401−7.
(89) Losi, M. E.; Frankenberger, W. T. Reduction of Selenium Oxyanions by *Enterobacter cloacae* SLD1a-1: Isolation and Growth of the Bacterium and Its Expulsion of Selenium Particles. *Appl. Environ. Microbiol.* **1997**, *63* (8), 3079−84.

(90) dos Reis, A. R.; El-Ramady, H.; Santos, E. F.; Gratão, P. L.; Schomburg, L. Overview of Selenium Deficiency and Toxicity Worldwide: Affected Areas, Selenium-Related Health Issues, and Case Studies. In *Selenium in Plants: Molecular, Physiological, Ecological and Evolutionary Aspects*; Pilon-Smits, E. A. H., Winkel, L. H. E., Lin, Z.-Q., Eds.; Springer International Publishing: Cham, 2017; pp 209−230.
(91) Yang, C.; Yao, H.; Wu, Y.; Sun, G.; Yang, W.; Li, Z.; Shang, L. Status and risks of selenium deficiency in a traditional selenium-deficient area in Northeast China. *Science of the total environment* **2021**, *762*, No. 144103.
(92) Tapiero, H.; Townsend, D. M.; Tew, K. D. The antioxidant role of selenium and seleno-compounds. *Biomedicine & Pharmacotherapy* **2003**, *57* (3−4), 134−144.
(93) Jones, G. D.; Droz, B.; Greve, P.; Gottschalk, P.; Poffet, D.; McGrath, S. P.; Seneviratne, S. I.; Smith, P.; Winkel, L. H. Selenium deficiency risk predicted to increase under future climate change. *Proc. Natl. Acad. Sci. U. S. A.* **2017**, *114* (11), 2848−2853.
(94) Gupta, M.; Gupta, S. An Overview of Selenium Uptake, Metabolism, and Toxicity in Plants. *Front Plant Sci.* **2017**, *7*, 2074.
(95) Zonaro, E.; Lampis, S.; Turner, R. J.; Qazi, S. J.; Vallini, G. Biogenic selenium and tellurium nanoparticles synthesized by environmental microbial isolates efficaciously inhibit bacterial planktonic cultures and biofilms. *Front Microbiol* **2015**, *6*, 584.
(96) Hariharan, H. N.; Karuppiah, P.; Rajaram, S. K. Microbial synthesis of selinium nanocomposite using *Saccharomyces cerevisiae* and its antimicrobial activity against pathogens causing nosocomial infection. *Chalcogenide Lett.* **2012**, *9*, 509−515.
(97) Sinha, S.; Kumar Chatterjee, S.; Ghosh, J.; Kumar Meikap, A. Semiconducting selenium nanoparticles: Structural, electrical characterization, and formation of a back-to-back Schottky diode device. *J. Appl. Phys.* **2013**, *113* (12), 123704.
(98) Schrauzer, G. N. Nutritional selenium supplements: product types, quality, and safety. *J. Am. Coll Nutr* **2001**, *20* (1), 1−4.

https://doi.org/10.1021/acsearthspacechem.2c00288
ACS Earth Space Chem. 2023, 7, 960−971